ELSEVIER

International Journal of Mass Spectrometry 190/191 (1999) 181–194

International Journal of Mass Spectrometry

A density functional theory study of the catalytic role of Ar, Kr, Xe, and N_2 in the $CH_3OH^{\cdot +}$ to $CH_2OH_2^{\cdot +}$ isomerization reaction

Travis D. Fridgen[a,b,1], J. Mark Parnis[a,b,*]

[a]*Department of Chemistry, Trent University, Peterborough, Ontario K9J 7B8, Canada*
[b]*Department of Chemistry, Queen's University, Kingston, Ontario K7L 3N6, Canada*

Received 25 August 1998; accepted 10 October 1998

Abstract

Density functional theory has been employed to investigate the influence of the neutral bases Ar, Kr, Xe and N_2 on the isomerization reaction of the methanol radical cation ($CH_3OH^{\cdot +}$) to its distonic isomer ($CH_2OH_2^{\cdot +}$). Results of all electron, BP86/DN** calculations predict that these neutral bases do catalyze this isomerization reaction. It is expected that, in the presence of Xe or N_2, this intramolecular H-atom transfer could be catalyzed efficiently, competing with the unimolecular dissociation channel which produces a hydrogen atom and the hydroxy methylene cation. Using theoretical data for four different isomerization reactions and numerous different catalysts, a linear relationship is found between the difference in proton affinities of the catalyst and the H-leaving site and the difference between the barrier heights of the uncatalyzed and catalyzed reactions, i.e. the lowering of the barrier. With this relationship, the decrease in the barrier height associated with a given base can be estimated, and the likely consequence of the coexistence of neutral base and hydrogen-containing cations in experiments can be assessed. It is further established that the density functional theory (DFT) methods and basis sets employed in this study do not predict very accurately the relative thermodynamic properties of the ionic species studied in this work. They do, however, give reasonable estimates of the decrease in energy because of association of a catalyst with the transition state. (Int J Mass Spectrom 190/191 (1999) 181–194) © 1999 Elsevier Science B.V.

Keywords: Density functional theory; Methanol medical cation ($CH_3OH^{\cdot +}$); Distonic isomer ($CH_2OH_2^{\cdot +}$); Catalysis

1. Introduction

The inter- and intramolecular mobility of the proton is of fundamental importance to the gas-phase chemical reactions of cationic species containing hydrogen. Proton mobility between molecules is at the heart of proton affinity studies and has been studied extensively by various mass spectrometric techniques [1,2]. It has been demonstrated that when the proton transfer between two species is exoergic, the reaction generally occurs readily [2,3] suggesting an insignificant energy barrier.

In contrast, energy barriers to intramolecular proton (or atom [4]) transfers are normally quite signif-

* Corresponding author (at Trent University).
[1] Present address: Department of Chemistry, University of Waterloo, Waterloo, Ontario N2L 361, Canada.

Dedicated to J.F.J. Todd and R.E. March in recognition of their original contributions to quadrupole ion trap mass spectrometry.

PII S1387-3806(98)14289-6

icant. This is best exemplified by the isomers of protonated carbon monoxide COH^+ and HCO^+ which have been individually isolated and characterized in the gas phase [5,6]. Isomerization in either direction is not observed to take place under normal experimental conditions and theory has shown there to be a very high energy barrier separating the two isomers [7,8]: 300 kJ mol^{-1} for the $HCO^+ \rightarrow HOC^+$ isomerization and 150 kJ mol^{-1} for the reverse process. It has been demonstrated, however, that significant HOC^+ to HCO^+ isomerization occurs in the presence of H_2 [9,10]. Theoretical calculations have shown that this is likely because of a catalytic reaction channel with a lower activation energy requirement involving a H_2-stabilized activated complex [10,11],

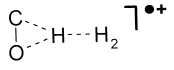

Diagram 1.

that is, H_2 acts to catalyze the isomerization. More recent theoretical studies demonstrate that many neutral species such as the rare gases, CO, HF, and H_2, etc. may also act to lower the barrier to such isomerization reactions [12,13] which Bohme has described as proton-transport catalysis [3].

Theorized in terms of proton-transport catalysis, two distinct mechanisms exist for the interaction of the catalyst with the shifting proton. When the leaving site has a lower proton affinity than the catalyst, and the accepting site a higher proton affinity than the catalyst, the proton may be transferred from the leaving site to the catalyst M forming a complex between the deprotonated precursor and MH^+. The proton is then transferred to the accepting site from MH^+, resulting in a "forth and back" proton shift isomerization [14] (Mechanism I). The energy requirement for this process is minimal because the barrier to intermolecular proton transfer is insignificant. This mechanism has proven to be consistent with recent experimental observations. In the CO or CO_2 catalyzed $HCN^+ \rightarrow HNC^+$ isomerization, Hansel [15] note that at higher temperatures catalysis is not as efficient. They explained the observed inverse temperature dependence to be the consequence of a shorter lifetime of the intermediate collision complex after the initial proton transfer from HCN^+ to CO (or CO_2).

In the second mechanism (Mechanism II), the catalyst has a lower proton affinity than both the proton leaving and accepting sites of the deprotonated molecule such that there is no proton transfer to the catalyst. Instead, the catalyst complexes with and stabilizes the transition-state structure, thereby lowering the activation energy barrier of the uncatalyzed reaction. Like the uncatalyzed reaction, this is a concerted bond-breaking/bond-making mechanism. The catalysts in this study (Ar, Kr, Xe, and N_2), have lower proton affinities than both the leaving and accepting sites for the $CH_3OH^{\cdot +} \rightarrow CH_2OH_2^{\cdot +}$ isomerization such that their reactions are examples of this form of catalysis.

For completeness we describe a third interaction which Gauld and Radom have described as the "spectator mechanism" [16] (Mechanism III), in which the catalyst is not directly involved in the migration of the proton, but is complexed at another position on the reacting cation. In this mechanism, the extent of catalysis is not as great as for the first two mechanisms, but may still lower the barrier with respect to the separated catalyst and reactant cation ($M + R^+$) compared to the isolated system. However, because stabilization of the complexed species ($M\cdots R^+$) is considerably greater, the barrier for isomerization of the complexed species is generally higher than that of its uncomplexed species in the isolated system.

As with HCO^+ and COH^+, the methanol radical cation ($CH_3OH^{\cdot +}$, **1**) and its distonic isomer ($CH_2OH_2^{\cdot +}$, **3**) have been individually observed. They do not interconvert and therefore must be separated by a large barrier [17,18]. Calculations have predicted this barrier to be slightly greater than 100 kJ mol^{-1} [19]. Experimentally, it has been shown that interaction of **1** with H_2O [20,21] or neutral methanol [21] facilitates the **1**↔**3** isomerization. High-level ab initio calculations [22] predict that when a "spectator" water molecule is bound to the hydroxy hydrogen, the barrier for interconversion with respect to complexed **1** and complexed **3** increases but lies slightly below the energy of separated H_2O and **1**. In contrast when

the water molecule interacts with the shifting proton, a barrier of only 15.9 kJ mol^{-1} above complexed **1** is predicted.

Quite recently, a theoretical survey of the effects of HF, H_2O, and NH_3 on the isomerization of $CH_3F^{\cdot+}$, $CH_3OH^{\cdot+}$, and $CH_3NH_2^{\cdot+}$ to their respective distonic isomers has been done by Gauld and Radom employing a modification of G2 theory [16]. In that paper, it is elegantly demonstrated that H_2O is ideally suited to catalyze the **1**↔**3** isomerization by Mechanism I, because its proton affinity lies between that of C and O in $CH_2OH^{\cdot}$. This is in contrast to hydofluoric acid (HF) which has a lower proton affinity than both ends of $CH_2OH^{\cdot}$ but still greatly reduces the energy barrier to isomerization (Mechanism II). NH_3 has a greater proton affinity than both ends and will not likely catalyze the **1**↔**3**, reaction but will more likely react to give NH_4^+ and $CH_2OH^{\cdot}$.

In this paper, we extend the work of Gauld and Radom to include the study of the effects of the nonpolar reagents Ar, Kr, Xe, and N_2 on the **1**–**3** isomerization. These gas-phase interactions can be of utmost importance in matrix isolation experiments where hydrogen-containing cations are in the presence of a great abundance of the aforementioned agents in the gas phase prior to condensation on the low-temperature substrate. Subsequently recorded spectra may reveal decomposition products of catalyzed isomerization rather than simple unimolecular decomposition products of energetic ionic species. Similarly, mass spectrometrists employ some of these species as collisionally induced dissociation (CID) agents and/or cooling agents in sector instruments and flow tubes as well as ion trap and ion cyclotron resonance (ICR) trap mass spectrometry, and therefore the possibility exists that catalytic isomerization may occur in these contexts.

2. Computational details

The accurate prediction of thermochemical quantities by G2, MP2, CBSQ (complete basis set-quadratic configuration interaction) and numerous DFT approaches to have recently been compared Curtiss et al. [23] and in numerous papers by Jursic [24–28]. Of these methods CBSQ ranks highest for accuracy followed closely by G2-related methods [24,25]. Hybrid DFT methods, although inferior to CBSQ and G2, also give very good results and, of these, the B3LYP method in conjunction with large Gaussian basis sets is particularly recommended. Although many of these procedures can be very accurate, they can be extremely time consuming. Furthermore, all-electron Gaussian basis sets for Kr and Xe are not readily available. The density functional method and numerical basis sets utilized in this study were chosen both for reasons of availability of reasonably large basis sets for Kr and Xe and for computational expediency.

All calculations were performed using the nonlocal spin density approximation (NLSDA) employing either Becke's gradient-corrected exchange functional (B) [29] or Becke's three parameter functional (B3) [30] combined with either of the gradient-corrected correlation functionals of Perdew (P86) [31], Lee, Yang, and Parr (LYP) [32] or Perdew and Wang PW91 [33]. The corrections to the local spin density gradient were recalculated at each step in the SCF iteration. The calculations were performed utilizing either a numerical double-ζ split-valence basis set with polarization functions added to all atoms including H (referred to as DN**) or the Gaussian double- or triple-ζ basis sets (6-31G*, 6-311G** or 6-311+G**) augmented with polarization functions on the heavy atoms (denoted with *) or on both the heavy atoms and H (**). Where the + symbol occurs in the basis set, diffuse functions were added to heavy atoms. The DN** basis set has been shown to give results comparable to those obtained using the 6-311G** Gaussian basis set used in conjunction with the same DFT functionals [34]. All calculations using the DN** basis set were performed using the SPARTAN 5.0 [35] set of programs and all calculations employing the Gaussian basis sets were performed using the GAUSSIAN 94W computational package [36]. The vibrational wavenumbers were calculated by numerical differentiation of analytical gradients (central differences).

3. Results

3.1. The uncatalyzed proton transfer

In this section, we report the results of the calculations performed on **1**, **3**, and the transition state joining them **2** employing three combinations of exchange and correlation functionals, namely BP86, B3PW91, and B4LYP with either the DN**, 6-31G*, 6-311G**, or 6-311+G** basis sets. These combinations of functionals in conjunction with the 6-31G* basis set were chosen in an attempt to extrapolate zero-point vibrational energy (ZPVE) and the vibrational component of the thermal contribution to enthalpy (ΔH_{vib} (298)) scaling factors for the BP86/DN** and other method/basis set combinations from those calculated by Scott and Radom [37]; these scaling factors could be used to correct the energies for systematic errors inherent in the computational methods. DFT calculated vibrational frequencies are generally quite good [37] resulting in scaling factors very close to 1 [38]. We found it unnecessary to correct the energies which follow because the corrected energies were the same, to a tenth of a kJ mol^{-1}, as those calculated without using scaling factors.

The BP86/DN** calculated structures of the methanol radical cation (**1**), its distonic isomer (**3**) and the transition state joining the two on the potential energy (**2**) surface are shown in Fig. 1. The geometries of these three cations compare quite well with those geometries found using the Gaussian basis sets. Similarly, the DFT-calculated geometries of all three species compare well with those obtained using HF, MP2, and QCISD(T) methods [19,39–41]. The most noteworthy difference with respect to geometries is that of **1**. Using HF, MP2, and QCISD, the symmetry of the calculated minima of the methanol radical cation are basis-set dependent. In most cases, the C_1 geometry is preferred with the HCOH dihedral angle about 16° from eclipsed [41] and the C_s structures being first-order saddle points on the potential energy surface. The results of all the DFT calculations reported here predict a C_s eclipsed geometry for **1** in agreement with QCISD(T)/6-311G* results [41] and MP2 results using the 6-311G**, 6-311+G**, 6-311G(2*df*,*p*) and 6-311+G(2*df*,*p*) basis sets [39]. Our calculated C–H(2) and C–H(3) bonds in **1** are 1.135 Å using BP86/DN**, considerably longer than normal C–H bond lengths. This is likely the result of the strong interaction between the oxygen $2p_x$ and $2p_z$ atomic orbitals and the C–H(2) and C–H(3) bonds which form the fourth highest occupied molecular orbital and which Tureček [42] and Ma et al. [19] have interpreted as hyperconjugative interaction in explaining the one longer C–H bond in their calculated C_1 structures of $CH_3OH^{\cdot+}$. These hyperconjugative interactions were also present in the C_s structures from references 39 and 41.

In Table 1 the enthalpies are listed for various stationary points on the $CH_4O^{\cdot+}$ potential energy surface. These calculated enthalpies are listed relative to the distonic isomer **3** for reasons discussed below. As has been asserted in the past [34], it is quite obvious that the DN** basis set yields similar results as the triple-ζ Gaussian basis using the same combination of exchange and correlation functionals. In fact, the BP86/DN** results are as good as the BP86/6-311+G** results from this point of view.

The most dissatisfying results of these calculations are associated with the energies of the methanol radical cation **1**. On examination of Table 1, it is clear that all of the DFT-calculated relative energies of **1** are in gross error when compared with both the G2 and experimental values. The best calculation is in error by 24 kJ mol^{-1}. In many cases **1** is calculated to be more stable than **3**, including all calculations employing BP86 theory; this is in direct contrast with experiment and all other methods of calculation. Comparing the proton affinities of the O and C ends of CH_2OH in the last column of Table 1 (C end proton affinities in the shaded column) it is recognized that the DFT methods employed here greatly overestimate the stability of the methanol radical cation. The calculated proton affinities of **3** are, however, in fairly good agreement with experiment and many of the barrier heights for the **1**↔**3** isomerization are in good agreement with the G2-calculated values.

The results of DFT calculations reported above have obvious problems with respect to the over stabilization of the methanol radical cation, however,

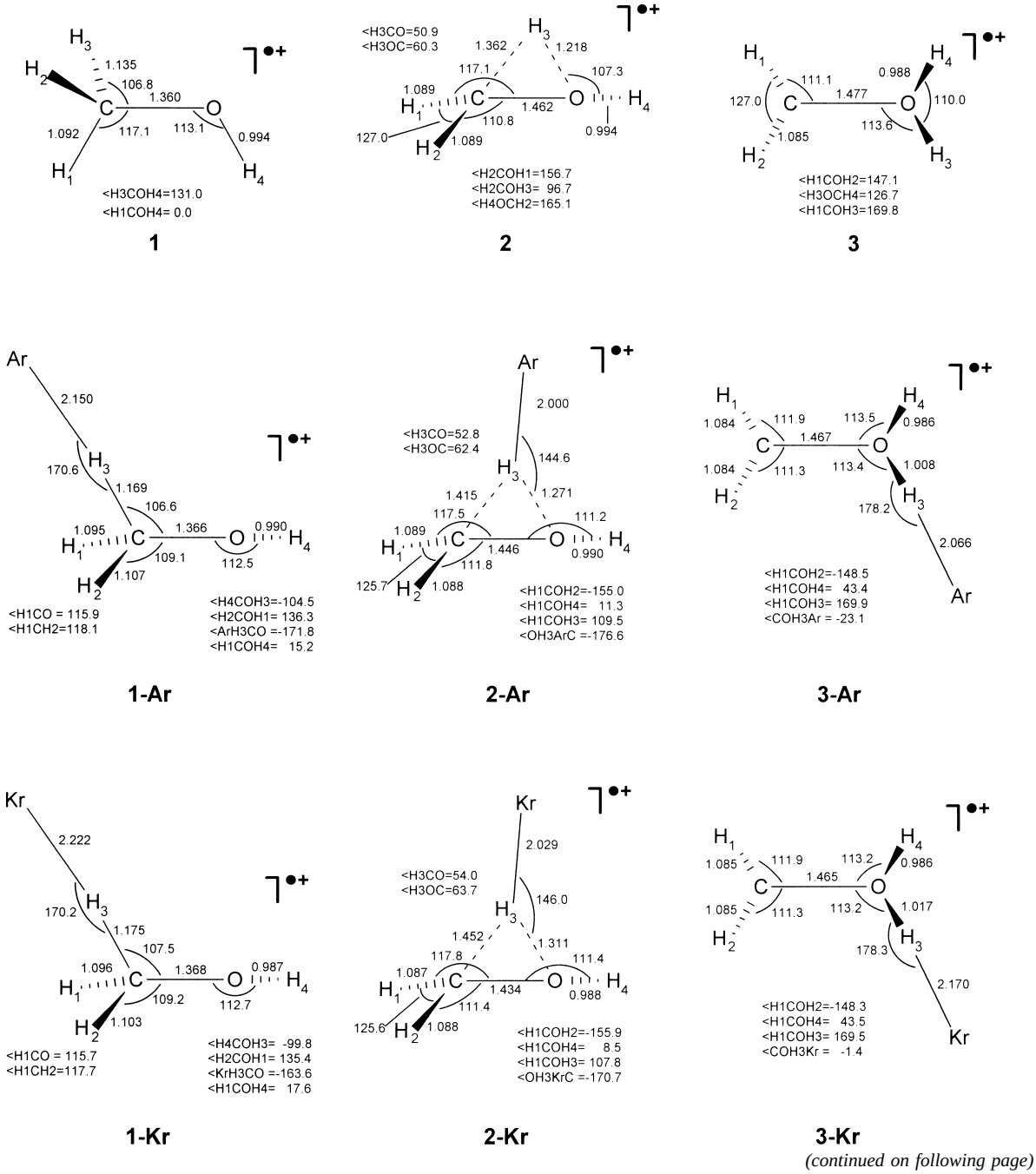

(continued on following page)

Fig. 1. BP86/DN** calculated geometries of the methanol radical cation (**1**), its distonic isomer (**3**), the transition state joining the two (**2**), and the Ar-, Kr-, Xe-, and N_2-associated species.

the primary values of interest here are the *differences* in barrier heights when Ar, Kr, Xe, or N_2 are complexed with the transition state. That the differences in barrier heights calculated here using BP86/DN** density functional theory are acceptable values is discussed below.

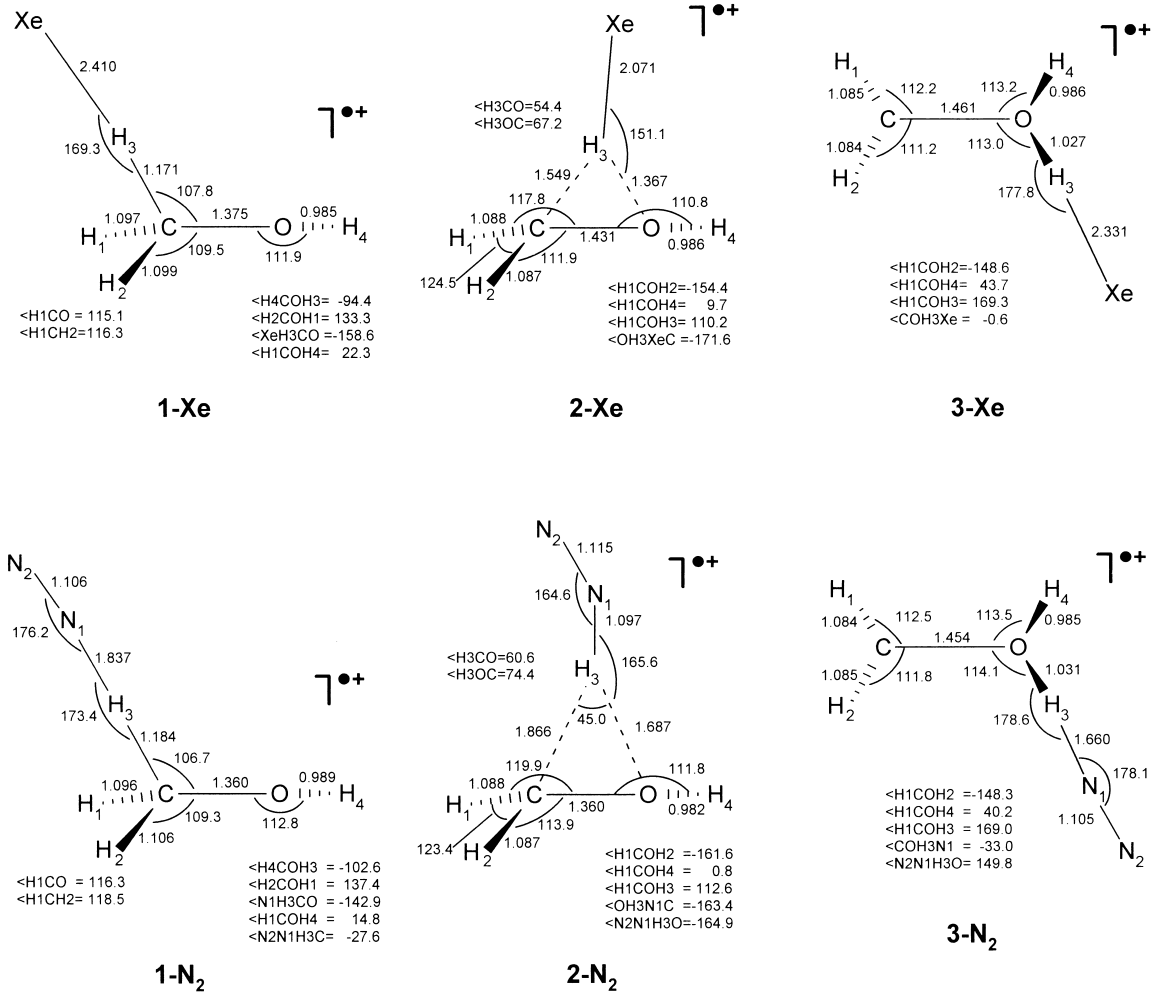

Fig. 1. *(continued from previous page)*

3.2. Ar-, Kr-, Xe-, and N_2-catalyzed proton transfer

In Table 2 the BP86/DN** and B3LYP/6-311+G** calculated relative energies of the stationary points in the Ar-catalyzed **1**–**3** isomerization are compared. As is the case for the uncatalyzed reaction and these two DFT method/basis set combinations (Table 1), the calculated energies do not agree. The calculated barrier heights are not in agreement, however, the decreases in barrier heights from the uncatalyzed reaction are predicted to be 18 and 12 kJ mol^{-1} for the BP86/DN** and B3LYP/6-311+G** calculations, respectively, differing by only 6 kJ mol^{-1}. Because we are primarily concerned with the difference between barrier heights we are confident in using the BP86/DN** DFT method to probe the effect of Ar, Kr, Xe, and N_2 on the barrier height of the **1**↔**3** proton transfer isomerization.

The BP86/DN** structures of the Ar-, Kr-, Xe-, and N_2-associated species of **1**, **2**, and **3** are shown in Fig. 1. The C–H(3) bond lengths of both **1-X** and **3-X** are seen to get progressively longer over the series X = Ar, Kr, Xe, or N_2. This increase seems reasonable as some degree of X–H bonding with a concomitant decrease in the order of C–H or O–H bonding is to be expected. This has also been observed in the

Table 1
Calculated and experimental 298 K relative[a] enthalpies (kJ mol^{-1}) for various stationary points on the $CH_4O^{\cdot+}$ potential energy surface

Method/basis set	$CH_3OH^{\cdot+}$ (**1**)	$H_2C(H)OH^{\cdot+}$ (**2**)	$CH_2OH_2^{\cdot+}$ (**3**)	$CH_2OH^{\cdot}$(**4**) + H^{+}[a]	
BP86/DN**	−10.2	115.7	0	685.0	695.2
BP86/6-31G*	−22.4	109.6	0	699.4	721.8
BP86/6-311G**	−10.6	111.3	0	700.8	711.4
BP86/6-311+G**	−10.2	111.5	0	686.7	696.9
B3LYP/6-31G*	−8.8	129.0	0	702.8	711.6
B3LYP/6-311G**	5.0	131.7	0	706.2	701.2
B3LYP/6-311+G**	5.6	131.9	0	691.7	686.1
B3PW91/6-31G*	−6.2	128.1	0	704.9	711.1
B3PW91/6-311G**	5.8	128.4	0	709.7	703.9
B3PW91/6-311+G**	6.3	130.1	0	697.6	691.3
G2[b]	31.8	135.7	0		
exptl[c]	30.3		0	689.1	658.8

[a] Energies in the darker columns are relative to $CH_3OH^{\cdot+}$, i.e. they correspond to the proton affinity of $CH_2OH^{\cdot}$ at C.
[b] From [19].
[c] Calculated using data from [47].

reports on catalyzed HCO^+ isomerization [13,16]. Note that the C–H(3) bond distance of **1-X**, however, shows a significant increase (0.034 Å) on going from **1** to **1-Ar** while the remaining two C–H bond lengths are quite normal, reflecting a strong interaction with the catalyst.

The results of these calculations, with respect to the energies, are shown graphically in Fig. 2. With respect to the **3-X** complexes, the barrier to isomerization does not decrease inordinately. However, with respect to (**X + 3**), the barrier decreases quite dramatically (that is, the net decrease in the barrier, with respect to separated reagents, is significantly reduced). Decreases of 18, 34, 55, and 65 kJ mol^{-1} are calculated for the Ar-, Kr-, Xe-, and N_2-catalyzed reactions, respectively. These catalyzed isomerization reactions become increasingly important, competing against the lower-energy decomposition pathway of **1** and **3** to form hydroxy methylene cation and hydrogen atom. It is important to note that the lowest energy pathways for decomposition of the $CH_4OX^{\cdot+}$ complex will be to form either of the $CH_4O^{\cdot+}$ isomers and X. Given enough energy and momentum along the appropriate reaction coordinate, however, it is still quite possible, to catalyze the **1**↔**3** isomerization. This has been considered as a possible source of mixed isotopomeric decomposition products in electron-bombardment matrix-isolation experiments conducted on methanol [43].

Table 2
Comparison of calculated stationary point energies along the Ar-catalyzed 1–3 isomerization

Stationary point	BP86/DN**	B3LYP/6-311+G**
Ar + 1	−10.2	5.6
Ar−1	−26.1	1.4
Ar−2	97.5 (−18)	119.9 (−12)
Ar−3	−14.6	−15.0
Ar + 3	0.0	0.0

Values in parentheses denote the difference between the respective calculated uncatalyzed barrier heights and the Ar-catalyzed barrier heights.

It can be seen by comparing the structures in Fig. 1 that the H(3)–X bond distances in the transition state (**2-X** species X = Ar, Kr, Xe, or N_2) are considerably shorter than in the **1-X** and **3-X** structures. This shorter bond distance can be thought of as owing to a strong interaction and stabilization of the transition structure. It is also apparent that the ratio of the H(3)–X bond distance in **2-X** to that in **1-X** (or **3-X**) decreases across the series Ar, Kr, Xe, N_2 which can be thought of as a greater stabilization of the transition structure across this series. Further evidence of this stronger interaction comes from the increasing H(3)–C and H(3)–O bond distances in the transition structures (**2-X**) over the same series; the H(3)–O bond distance increases from 1.218 Å in the unasso-

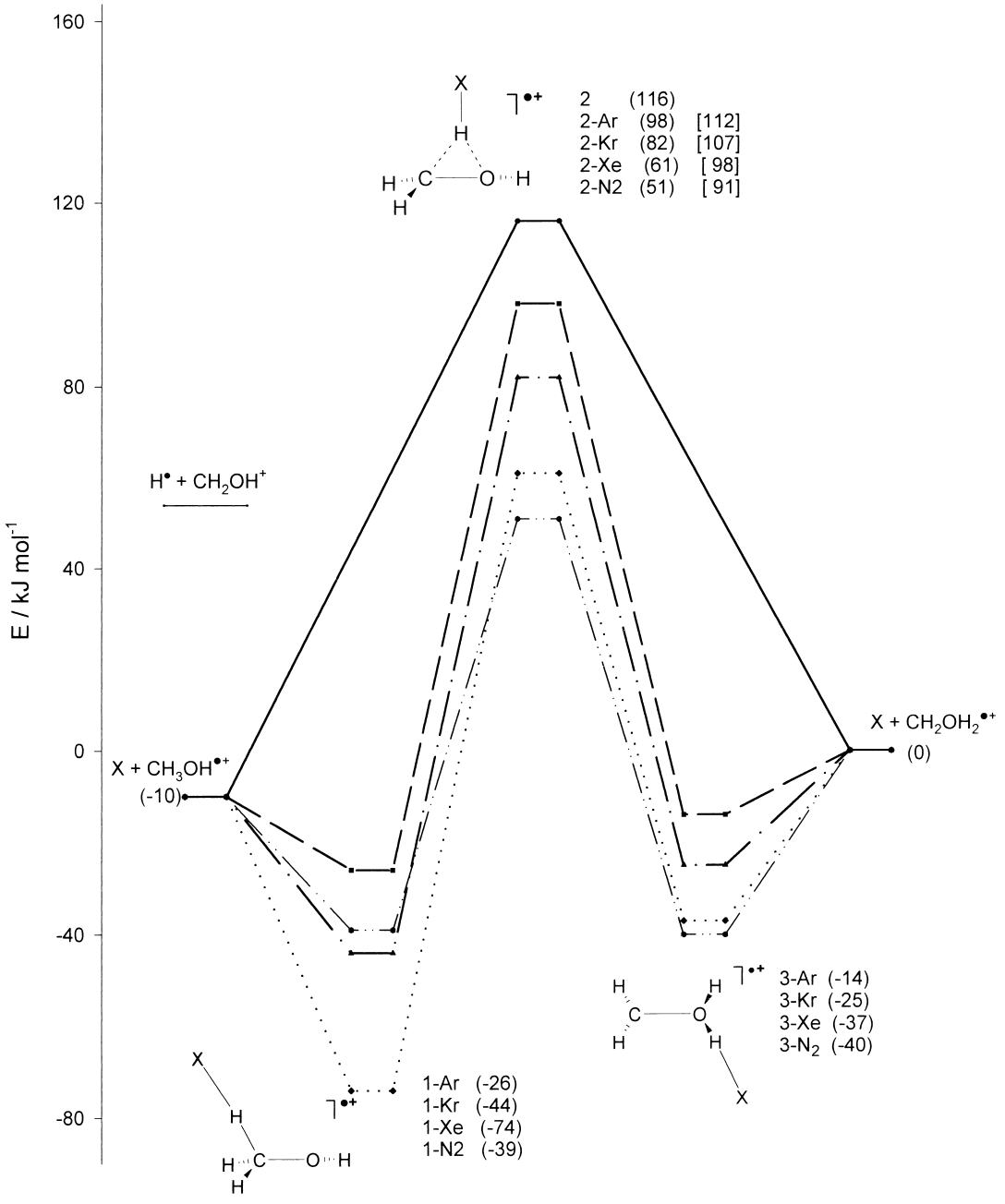

Fig. 2. Schematic 298 K energy profile showing the uncatalyzed isomerization (solid line), and the Ar, Kr, Xe, and N_2 catalyzed isomerization reactions (dashed line, dash-dot line, dotted line, and dash-dot-dot line, respectively). The values in squared parentheses denoted the barrier height with respect to the complexes **3-X**. Energy of $H^- + CH_2OH^+$ from [19].

ciated structure (**2**) to 1.271, 1.311, 1.367, and 1.687 Å for the Ar-, Kr-, Xe-, and N_2-associated transition structures, respectively (see also Fig. 3).

We may also gain insight into the stabilization of the transition state by the catalysts by looking at the charge distributions. The charge distributions ob-

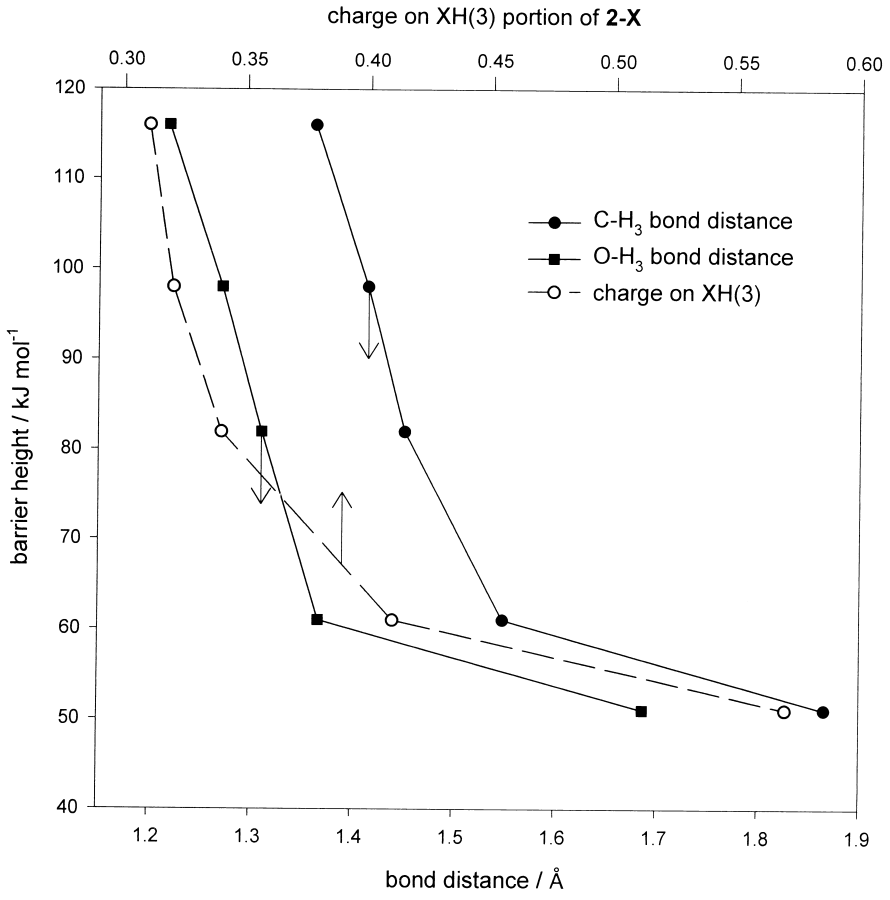

Fig. 3. Plot showing the relationship of the barrier heights of the catalyzed and uncatalyzed **1**–**3** H-atom transfers with the C–H(3) and O–H(3) bond lengths in the predicted transition state, and the charge on the XH(3) portion of the transition state. The abscissa for the latter of these is at the top of the plot.

tained from the electrostatic potentials show that on average 31% of the charge is on H(3) of the uncatalyzed transition state, **1**, while in the Ar-, Kr-, Xe-, and N_2-stabilized transition states 32, 34, 41, and 57% of the charge is on the XH(3) portion, respectively (Fig. 3). This increase in charge on the XH(3) portion of the transition state is associated with an increase in positive charge on the catalyst. The average charge associated with H(3) decreases from 31% on the uncatalyzed transition structure to 14, 6, and 1% in the Ar-, Kr-, and Xe-stabilized transition state and is 16% in the N_2-stabilized structure. Thus, on the X portion, the charge increases from 18% when X = Ar to 28, 40, and 41% when X = Kr, Xe, and N_2, respectively. The charges on the catalysts in the respective transition states are plotted in Fig. 4 against their proton affinities and a good linear relationship is obtained. It should be noted here that although the isomerization reactions discussed in this paper have been given the unfortunate misnomer "intramolecular proton transport," the identity of the migrating substituent more closely resembles that of a hydrogen atom in both the catalyzed and uncatalyzed reactions. Therefore, from here on the process will be referred to as intramolecular H-atom transport.

With respect to the unpaired spin density, all transition states closely resemble $CH_2OH_2^{\cdot+}$ in that the radical centre is mostly on C. Neither the catalyst nor

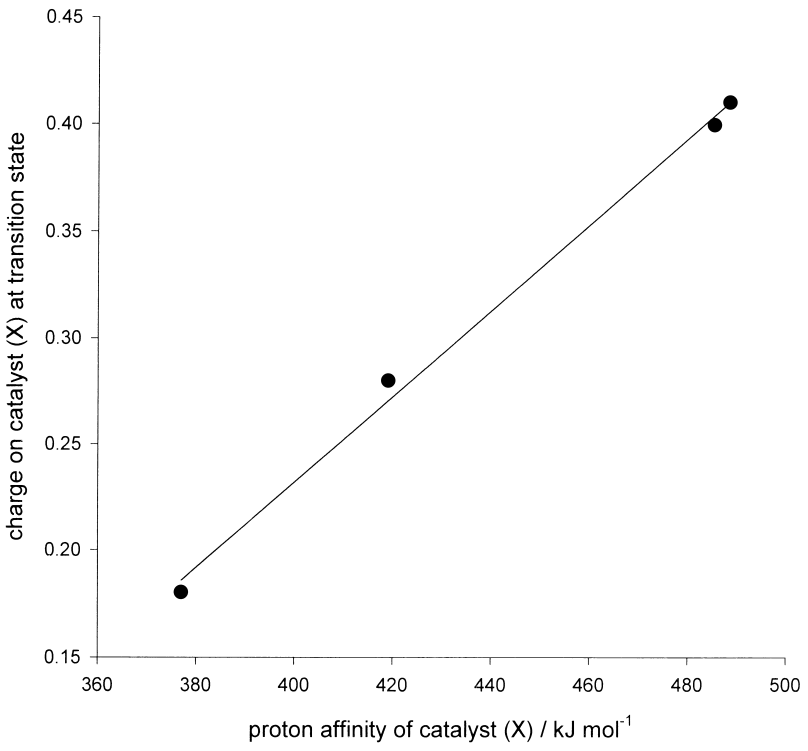

Fig. 4. Plot showing the relationship between the calculated proton affinities and the calculated charge on the catalyst (X) derived from the electrostatic potentials.

H(3) have any appreciable unpaired spin density consistent with a net transfer of charge to the stabilized ion from the catalyst through the H atom. In $CH_3OH^{\cdot+}$, the spin density is more evenly distributed between C and O but, is still slightly greater on C. Because there is some extent of transfer of spin density from O to C, the reaction may also involve some degree of electron transfer but, this transfer is complete before the transition state is reached.

4. Discussion

4.1. Catalyzed proton transfer

In the work by Chalk and Radom [12] it was realized that the calculated barrier height of the catalyzed isoformyl cation to formyl cation rearrangement decreased as the proton affinity of the catalyst increased. Similarly, the relationship between proton affinity of the catalyst and the charge distribution on the catalyst in the transition state depicted in Fig. 4 strongly suggests a linear relationship. In Fig. 5, we have plotted the difference between the uncatalyzed barrier height and the catalyzed barrier height (ΔBH, for change in barrier height) versus the difference between the proton affinities of the catalyst and the leaving sites of the proton (ΔPA) [44]. It is immediately apparent that there is a convincing linear relationship between ΔBH and ΔPA. This linear relationship is even more striking when one considers that there are data from four different 1,2-proton shift isomerization reactions and 12 different catalysts in Fig. 5. The vertical line denotes where the proton affinities of the leaving site and the catalyst are equal ($\Delta PA = 0$). To the left of this line ($\Delta PA < 0$) the catalysts may act by stabilizing the transition structures as in mechanism II. To the right ($\Delta PA > 0$) the catalysts may act by the “forth and back” mechanism

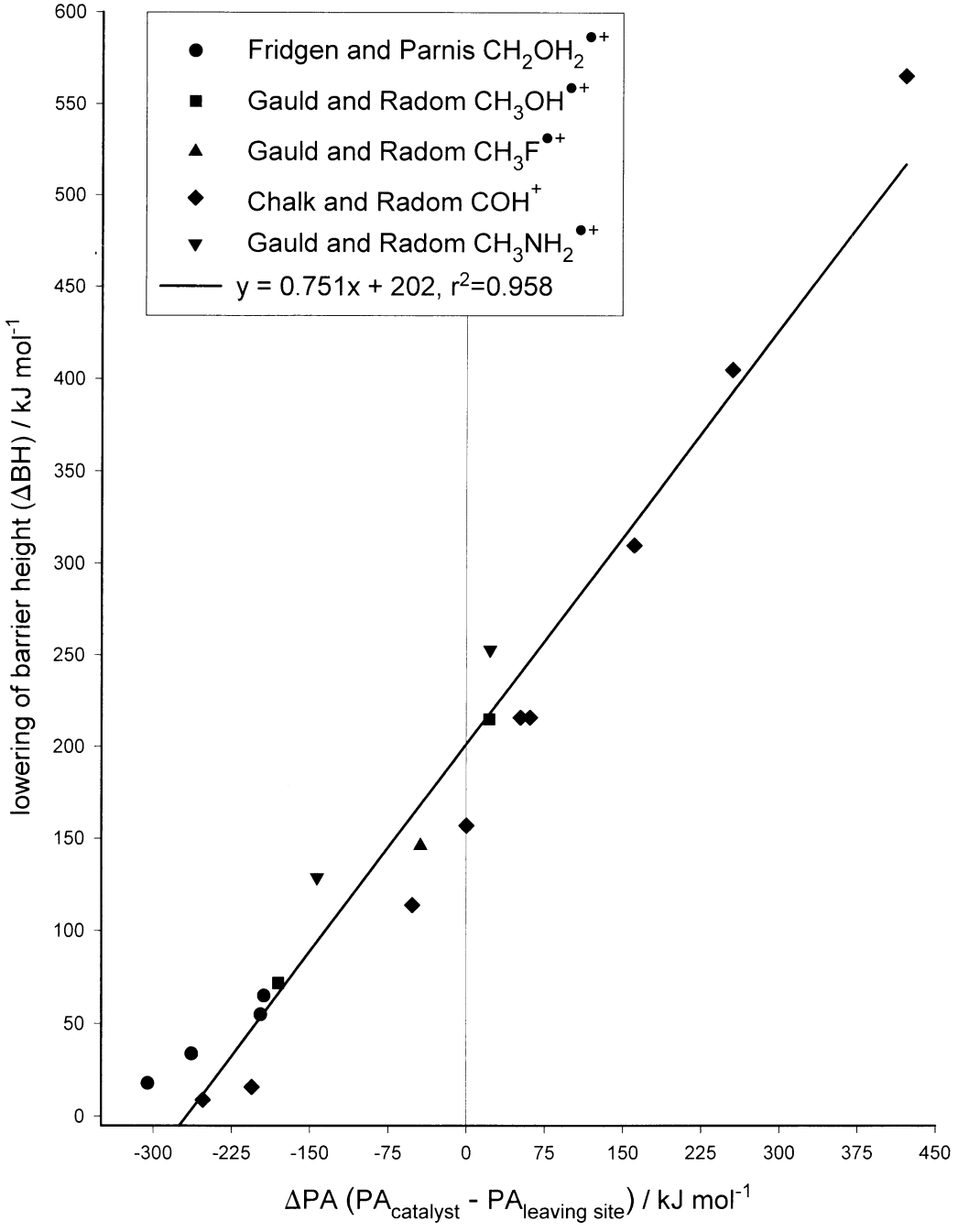

Fig. 5. Plot of the lowering of the barrier height (ΔBH) against the difference in proton affinities of the catalyst and leaving site (ΔPA) for various 1,2-H atom shift isomerization reactions and various catalysts. Data taken from [12] (◆), [16] (■,▲,▼), and this work (●). The points to the left of the vertical line represent catalyzed reactions where the proton affinity of the catalyst is less than the leaving site and, therefore, the catalyst simply stabilizes the transition structure.

or, for high proton affinity catalysts, may actually extract the proton (intermolecular proton transfer).

This correlation suggests that one could easily assess the extent of barrier lowering that is possible and by what mechanism it may effect the outcome of a given experiment by knowing or given reasonable estimates of the proton affinities of the leaving site and the neutral base. For example, in experiments designed to measure rates of reactions involving hydrogen-containing cations or to measure branching ratios of competing reactions, this correlation could be used to assess the possibility of catalysis of isomerization as an intermediate step before dissociation and to determine the likely mechanism. It also has value in the context of using appearance potential measurements to get at thermodynamic properties where neutral bases present as an "inert" bath or as an impurity, may catalyze isomerization.

We now recognize that rare-gas catalyzed H-atom transfer is likely to be an active mechanism in two of our recent electron bombardment matrix isolation (EBMI) studies. In work by Zhang et al. [45], 1-propen-2-ol was isolated and spectroscopically characterized in rare-gas matrices following periods of electron bombardment of gaseous rare gas/acetone mixtures (EBMI). It was assumed that the 1-propen-2-ol observed was the neutralized isomerization product of the *electronically excited* (*A* state) acetone radical cation. This *A* state mechanism arose because of the fact that the barrier to isomerization of the acetone radical cation to the 1-propen-2-ol radical cation is $\sim$71 kJ mol^{-1} higher in energy than the lowest energy dissociation into the acetyl cation and methyl radical [46], making isomerization of the cation in the ground state highly unlikely. The acetone radical cation to 1-propen-2-ol radical cation H-atom shift isomerization is not a 1,2-shift as is the **1**$\leftrightarrow$**3** isomerization, but is a 1,3-H atom shift. We recognize that use of Fig. 5 for this system is only of qualitative value, however, one may expect that the mechanisms to catalysis should be similar for 1,3- and 1,2-H-atom shifts. BP86/DN** calculations predict the ΔPA for Ar and the carbon site of $CH_3C(O)CH_2$ to be -403 kJ mol^{-1}. From Fig. 5 one can presume that the argon present in these experiments would have little or no effect on the barrier height. In fact for catalysis by Ar, preliminary calculations predict that the barrier is lowered from the parent system by only about 1 kJ mol^{-1}. However, there are expected to be many other neutral bases present such as CO and H_2O (impurities and products) which have proton affinities that differ from that of $CH_3C(O)CH_2$ at the carbon site by much less, -189 and -100 kJ mol^{-1}, respectively. The extent of catalysis is estimated from Fig. 4 to be 60 and 127 kJ mol^{-1} for CO and H_2O, respectively. Both CO and H_2O would be expected, therefore, to stabilize the transition structure, thereby lowering the barrier such that the dominant process could be isomerization of the acetone radical cation to 1-propen-2-ol radical cation. Thus, such catalysis may be a plausible mechanism for the isomerization of acetone observed by Zhang et al. Detailed calculations aimed at assessing the catalytic effect of various neutral bases on 1,3 H-atom shifts are currently underway.

In a more recent communication we concluded that the presence of species such as HDCO and $D_2COD^{\cdot}$ in rare gas matrices after EBMI of gaseous mixtures of D_3COH diluted in rare gases was a result of a gas-phase decomposition of the isotopically labeled methanol radical cation following Ar-catalyzed proton transfer to the more thermodynamically stable distonic cation [43]. The barrier to isomerization of the methanol radical cation is expected to be about 43 kJ mol^{-1} higher in energy than the lower energy dissociation to CH_2OH^+ and $H^{\cdot}$ [19]. Because Ar is only expected to lower the isomerization barrier by about 18 kJ mol^{-1} it may not be as likely that Ar is the catalyzing species, but rather impurities such as N_2, CO, or H_2O. In experiments where Kr or Xe replaced Ar as the diluent gas, it is also expected that they would catalyze the isomerization, although in that study the mixed isotope experiments were not conducted with Kr or Xe as the diluent gas.

4.2. The density functional approach

It is quite obvious that there are some serious difficulties with employing even the best of the density functional theory approaches in attempting to

predict thermodynamic and kinetic quantities for the ionic reactions presented in this paper.

With respect to calculated energies the BP86 method fails as is evidenced by the relative energies of **1** and **3** on comparison with experimental and G2 values. The B3LYP and B3PW91 values are in better agreement using the triple-ζ Gaussian basis sets, at least correctly predicting the proper ordering of the energies of the **1** and **3** isomers. It is important to note that there is little difference in the calculated energies by the addition of diffuse functions to the triple-ζ basis sets. These relative energies and proton affinities of **1**, however, are still not very reliable values employing any of the methods presented here. Obviously, the G2 values are quite superior. However, the calculations with the Gaussian basis sets were performed on a 200 MHz PC with 32 MB of RAM. G2 calculations would be impossible to perform with such modest computer facilities. We do maintain, however, that these DFT calculations accurately predict the expected trend in Ar, Kr, Xe, and N_2 catalytic effects of the **1**↔**3** isomerization, as evidenced by the fact that our results, plotted in Fig. 5, are in line with the G2 results from Radom's group.

5. Conclusions

The calculations presented here show that rare gases and N_2 can indeed catalyze the $CH_3OH^{\cdot+}$ to $CH_2OH_2^{\cdot+}$ 1,2-H atom transport isomerization. The presence of Xe and N_2 may very well result in a catalytic effect such that the isomerization of the methanol radical cation to the distonic isomer competes against the lowest energy dissociation route which produces a hydrogen atom and the hydroxy methylene cation. In this work, the theoretical results of other groups as well as our own has been used to show that there is a linear relationship between the difference in proton affinities of neutral base (catalyst) and the H leaving site of a radical cation (ΔPA) and the barrier lowering of the isomerization process with respect to the separated base-cation pair (ΔBH). This effect of neutral bases, either as bath gases or impurities, should be considered seriously when conducting experiments with hydrogen-containing cations. Further experiments designed to test the theoretical results provided here need to be designed. Similarly, experimental and theoretical work needs to be conducted on 1,3- and 1,4-H atom shift isomerization reactions.

It has also been shown that, although DFT methods are for the most part inferior to other computational modeling methods, fairly good results can be obtained with respect to the catalytic processes described in this paper. Further development of the DFT models used here needs to be done with respect to ionic potential energy surfaces before they will be useful in quantitative prediction of thermodynamic properties of ionic systems.

Acknowledgements

The careful reading of the manuscript by Professor E.G. Lewars is greatly appreciated. The valuable comments from the referee were very much appreciated and were quite instrumental in formulating the final draft of the manuscript. The authors wish to express their gratitude for the financial assistance provided by NSERC and Queen's University. We would like to extend our sincerest congratulations to Professor R.E. March in his retirement and TDF would like to thank him for invaluable encouragement and instruction over the past 10 years.

References

[1] For example see (a) M.N. Glukhovtsev, J.E. Szulejko, T.B. McMahon, J.W. Gauld, A.P. Scott, B.J. Smith, A. Pross, L. Radom, J. Phys. Chem. 98 (1994) 13 099; (b) J.E. Szulejko, T.B. McMahon, J. Am. Chem. Soc. 115 (1993) 7839.
[2] For example (a) D.K. Bohme, G.I. Mackay, H.I. Schiff, J. Chem. Phys. 73 (1980) 4976; (b) D.K. Bohme, Trans. R. Soc. Can. Sect. 3 19 (1981) 265.
[3] D.K. Bohme, Int. J. Mass Spectrom. Ion Processes 115 (1992) 95.
[4] Strictly speaking this process is not a proton transfer, as it is commonly referred to in the literature. It is in fact an H-atom transfer. This point is addressed later in the paper.
[5] C.S. Gudeman, R.C. Woods, Phys. Rev. Lett. 48 (1982) 1344.

[6] R.C. Woods, T.A. Dixon, R.J. Saykally, P.G. Szanto, Phys. Rev. Lett 35 (1975) 1269.
[7] R.H. Nobes, L. Radom, Chem. Phys. 60 (1981) 1.
[8] Y. Yamaguchi, C.A. Richards Jr., H.F. Schaefer III, J. Chem. Phys. 101 (1994) 8945.
[9] C.G. Freeman, J.S. Knight, J.G. Love, M.J. McEwan, Int. J. Mass Spectrom. Ion Processes 80 (1987) 255.
[10] W. Wagner-Redeker, P.R. Kemper, M.F. Jarrold, M.T. Bowers, J. Chem. Phys. 83 (1985) 1121.
[11] D.A. Dixon, A. Komornicki, W.P. Kraemer, J. Chem. Phys. 81 (1984) 3603.
[12] A.J. Chalk, L. Radom, J. Am. Chem. Soc. 119 (1997) 7573.
[13] A. Cunje, C.F. Rodriquez, D.K. Bohme, A.C. Hopkinson, J. Phys. Chem 102 (1998) 478.
[14] E.E. Ferguson, Chem. Phys. Lett 156 (1989) 319.
[15] A. Hansel, M. Glantschnig, Ch. Scheiring, W. Lindinger, E.E. Ferguson, J. Chem. Phys. 109 (1998) 1743.
[16] J.W. Gauld, L. Radom, J. Am. Chem. Soc. 119 (1997) 9831.
[17] W.J. Bouma, J.K. McLeod, L. Radom, J. Am. Chem. Soc. 104 (1982) 2930.
[18] J.L. Holmes, F.P. Lossing, J.K. Terlouw, P.C. Burgers, J. Am. Chem. Soc. 104 (1982) 2930.
[19] N.L. Ma, B.J. Smith, J.A. Pople, L. Radom, J. Am. Chem. Soc. 113 (1991) 7903.
[20] P. Morgues, H.E. Audier, D. Lablanc, S. Hammerum, Org. Mass Spectrom. 28 (1993) 1098.
[21] H.E. Audier, D. Leblanc, P. Morgues, T.B. McMahon, S. Hammerum, J. Chem. Soc. Chem. Commun. (1994) 2329.
[22] J.W. Gauld, H. Audier, J. Fossey, L. Radom, J. Am. Chem. Soc. 118 (1996) 6299.
[23] L.A. Curtiss, P.C. Redfern, K. Raghavachari, J.A. Pople, J. Chem. Phys. 109 (1998) 42.
[24] B.S. Jursic, Chem. Phys. Lett 284 (1998) 281.
[25] B.S. Jursic, Theor. Chem. Acc. 99 (1998) 171.
[26] B.S. Jursic, Theochem. 423 (1998) 189.
[27] B.S. Jursic, Theochem. 418 (1997) 11.
[28] B.S. Jursic, Theochem. 417 (1997) 89.
[29] A.D. Becke, Phys. Rev. A 38 (1988) 3098.
[30] A.D. Becke, J. Chem. Phys. 98 (1993) 5648.
[31] J.P. Perdew, Phys. Rev. B 33 (1986) 8822.
[32] C. Lee, W. Yang, R.G. Parr, Phys. Rev. B 37 (1988) 785.
[33] J.P. Perdew, Y. Wang, Phys. Rev. B 45 (1992) 13 244.
[34] A Guide to Density Functional Calculations in SPARTAN, W.J. Hehre, L. Lou, (Eds.), Wavefunction, Inc.: Irvine, 1997.
[35] SPARTAN Version 5.0, Wavefunction, Inc., 18401 Von Karman Avenue, Suite 370, Irvine, CA 92612, USA.
[36] GAUSSIAN 94, Revision E.1, M.J. Frisch, G.W. Trucks, H.B. Schlegel, P.M.W. Gill, B.G. Johnson, M.A. Robb, J.R. Cheeseman, T. Keith, G.A. Petersson, J.A. Montgomery, K. Raghavachari, M.A. Al-Laham, V.G. Zakrzewski, J.V. Ortiz, J.B. Foresman, J. Cioslowski, B.B. Stefanov, A. Nanayakkara, M. Challacombe, C.Y. Peng, P.Y. Ayala, W. Chen, M.W. Wong, J.L. Andres, E.S. Replogle, R. Gomperts, R.L. Martin, D.J. Fox, J.S. Binkley, D.J. Defrees, J. Baker, J.P. Stewart, M. Head-Gordon, C. Gonzalez, J.A. Pople, Gaussian, Inc., Pittsburgh, PA, 1995.
[37] A.P. Scott, L. Radom, J. Phys. Chem. 100 (1996) 16 502.
[38] Scaling factors of 1.005 (±0.004) and 1.016 (±0.003) were obtained for the ZPVE's for the BP86/DN** and BP86/6-311G** methods, respectively. Similarly, scaling factors for ΔH_{vib} (298) were calculated to be 1.00(±0.05) and 0.98(±0.08) for the BP86/DN** and BP86/6-311G** methods, respectively.
[39] J.W. Gauld, L. Radom, J. Phys. Chem. 98 (1994) 777.
[40] N.L. Ma, B.J. Smith, L. Radom, J. Phys. Chem. 96 (1992) 5804.
[41] B.F. Yates, W.J. Bouma, L. Radom, J. Am. Chem. Soc. 109 (1987) 2250.
[42] F. Tureček, Int. J. Mass Spectrom. Ion Processes 108 (1991) 137.
[43] T.D. Fridgen, J.M. Parnis, J. Chem. Phys. 109 (1998) 2155.
[44] The proton affinity of the leaving site is defined as follows, for the $CH_3OH^{\cdot+}$ to $CH_2OH_2^{+}$ isomerization it is the proton affinity of $CH_2OH^{\cdot}$ at carbon. For the reverse isomerization it would be the proton affinity of $CH_2OH^{\cdot}$ at oxygen. Similarly for the other reactions denoted in Fig. 4.
[45] X.K. Zhang, J.M. Parnis, E.G. Lewars, R.E. March, Can. J. Chem. 75 (1997) 276.
[46] T.H. Osterheld, J.I. Brauman, J. Am. Chem. Soc. 115 (1993) 10 311.
[47] S.G. Lias, J.E. Bartress, J.F. Liebman, J.L. Holmes, R.D. Levin, W. Mallard, J. Phys. Chem. Ref. Data 17 (1988) Suppl. 1.